Synthesis and Spin-Transport Properties of Co/Cu Multilayer Nanowires

Peter Greene*

Department of Physics, University of Washington, Seattle, Washington, 98105†

(Dated: October 10, 2007)

Using a combination of argon ion sputtering and electrodeposition, I fabricated multilayered Co/Cu nanowires in nuclear track etched, polycarbonate membranes of varying pore diameters. The confined geometry of the nanowires allowed me to study nanomagnetic properties along with current perpendicular to plane giant magnetoresistance (CPP-GMR). I also extended the measurement technique of First Order Reversal Curves (FORCs) to GMR.

I. INTRODUCTION

Nanomagnets have become increasingly important in modern day technological applications and the mechanisms that govern them warrant further investigation. Nanoferromagnets behave quite differently than macroscopic ferromagnets in terms of domain structure and reversal mechanisms. The actual determination of these structures and the reversal mechanisms involved is quite complex. Conventional magnetometry techniques are, in general, not sensitive enough to probe individual nanostructures. Furthermore, techniques that are sensitive to these small scales are often not able to access the samples due to the geometry of the heterogeneous structure.

II. BACKGROUND

In a macroscopic ferromagnet the magnetic structure is accurately described by the domain theory of magnetism [1]. The energy associated with a ferromagnet can be broken into several terms: field, anisotropy, and exchange. The magnetostatic energy is the integral over all space, $\frac{1}{2\mu_0} \int B^2 dV$ in SI units. For macroscopic ferromagnets it then becomes energetically favorable to have domains that reduce or eliminate the stray magnetic field outside of the ferromagnet's boundaries. However there is an energy cost associated with having neighboring moments at an angle to each other. Exchange energy favors parallel magnetic moment alignment and so a finite amount of energy is required to form a domain wall[1]. Furthermore, for crystalline structures, there are easy and hard axes of magnetization. This is referred to as magnetocrystaline anisotropy. Depending on the particular element and crystalline structure some directions require more energy to saturate the magnetization than others. Hence, domains oriented along a hard axis in a single crystal structure would be more energetically costly than if they were oriented along an easy axis. The number and relative orientation of the easy and hard axes is completely determined by the symmetry of the crystal and the electron structure of the element or compound. Additionally, even for polycrystalline structures, there is an anisotropic energy associated its shape. This field is called the demagnetization field $H_d = NM$ where M is the magnetization and N is the demagnetization factor whose components satisfy $N_x + N_y + N_z = 4\pi$ in CGS units. For an infinitely thin, infinite rod oriented along the z axis, the demagnetization field is zero along the rod $N_z = 0$. Then by symmetry we can easily conclude that $N_x = N_y = 2\pi$. Likewise a sphere has $N_x = N_y = N_z = \frac{4\pi}{3}$ and an infinitely thin disk has $N_x = N_y = 0$ in plane, $N_z = 4\pi$[2]. The easy axis for this shape anisotropy is then the direction with the lowest demagnetization field value. The ultimate ground state is a global optimization of all these factors.

The critical length scale for ferromagnets is the typical domain wall width $\delta = \pi \sqrt{\frac{A}{K}}$[2] where A is the exchange stiffness and K is the magnetocrystaline anisotropy constant of the lattice. For a typical ferromagnet this width is on the order of nanometers. For bulk ferromagnets it becomes energetically favorable to form multiple domain walls and minimize the external magnetic field as the domain wall energy scales with the area and the magnetic field energy scales with the volume[2]. As the dimensions of the particle reach the nanoscale, the energy associated with domain wall formation becomes larger than the energy of the external field and a single domain structure is realized. This is characterized by all the magnetic moments being aligned along a particular direction. Between the scale of single domain and multidomain states a vortex state domain configuration is often obtained. This state is typically accessed when the size of the magnetic particle is approaching to the domain wall width, and is most easily found in a disk geometry. As the field is reversed from positive saturation instead of the domain coherently rotating as a whole, as would happen in the single domain case, the domain "buckles" and the moments begin to curve into a crescent pattern as is shown in FIG. 1. The chirality is a case of spontaneous symmetry breaking and is random for perfect disks. The exchange energy is the angle determined between adjacent moments. When reversing from positive saturation, as the moments in the disk begin to curl, the angle between adjacent moments at the center of curvature would become very large if the moments stayed in the plane of the disk. To minimize this angle, the moments tilt progressively more out of plane as the curvature becomes

greater and greater until a vortex core is established at the center of curvature, this field strength is called the nucleation field. The vortex core has its moments pointing perpendicular to the plane of the disk. The direction of the vortex core moments is another case of spontaneous symmetry breaking and is random for symmetric disks under a large reversal field. The vortex core then travels across the disk, perpendicular to the direction of the applied field, and at the center there is complete flux closure within the plane of the disk. It continues across the disk until the core annihilates at the annihilation field. The curved moments straighten out as the field is further decreased and negative saturation is achieved when they all align.
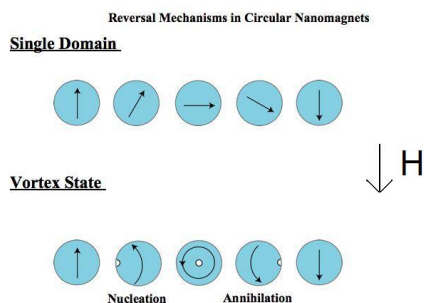

FIG. 1: Single domain vs. vortex state reversal mechanisms under a reversal field H

Giant magnetoresistance effects, subject of this year's Nobel Physics Prize[3][4], are encountered when magnetic layers are separated by conductive spacers on length scales of nanometers and current is passed through the structure. The current may be passed either along the layers or through the layers. For this paper we will only discuss the relevant case of current perpendicular-to-plane giant magnetoresistance (CPP-GMR). When small cobalt disks are brought close together they experience either ferromagnetic or antiferromagnetic coupling with an oscillatory dependence on the seperation between the disks[5]. Antiferromagnetic coupling is when adjacent moments(disks) align antiparallel to each other. For CPP-GMR studies, perfect antiferromagnetic coupling is ideal for reasons that will become clear. Currents passed through layered magnetic structures can be decomposed into two spin polarized currents[6] aligned parallel or antiparallel to the magnetization of the layer. The spin polarized current aligned parallel to the direction of magnetization has a lower resistance than the opposite polarization. At low fields the magnetic layers align antiferromagneticly and both spin polarized currents see alternating layers of low and high resistance. At high fields the layers are forced into ferromagnetic alignment and one spin polarized current sees low resistance while the other sees high resistance and most of the current is shunted through the low resistance channel[6]. This causes a lower total resistance state and gives rise to the phenomenon known as GMR. These effects are only seen below the critical length scale known as the spin flip diffusion length[6][7]. The spin flip diffusion length is the length at which a spin polarized current undergoes enough spin flip scattering events that the initial polarization is lost and is on the order of nanometers[7].

III. SAMPLE FABRICATION

I fabricated multilayered Co/Cu nanowires of varying diameters using a variety of techniques. The template for the nanowires was nuclear track etched polycarbonate membranes with pore diameters of 50, 100, and 200 nanometers. The polycarbonate membranes are exposed to a nuclear radiation source. The radiation causes tiny defects in the polycarbonate which is then exposed to a chemical etchant. The etchant dissolves the damaged polycarbonate much faster than the undamaged sections and small tracks are left that go straight through the membrane. I placed the membranes in an argon ion sputtering chamber to coat them with copper. The chamber is pumped out to ultra high vacuum (10^{-8} Torr). Argon is then introduced and the pressure is kept in the mTorr range. Argon atoms are ionized and accelerated by an applied voltage toward copper targets. The kinetic energy of the argon ejects copper atoms which then deposit onto the membrane. The trajectories of the copper ions are roughly isotropic over the area of the membrane so instead of filling the pores, the copper caps and seals the membrane. This copper film is then used as the working electrode in the electrodeposition stage of the sample fabrication.
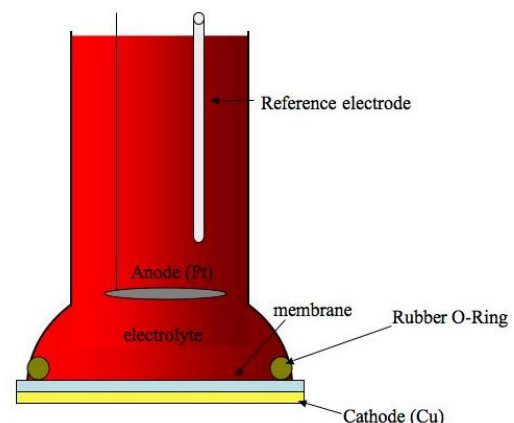

FIG. 2: Electrodeposition Cell

I used a standard three electrode electrodeposition setup consisting of a $Ag^+/AgCl$ reference electrode, a Pt mesh counter electrode (anode), and the Cu working

electrode (cathode) shown schematically in FIG. 2. All voltages are measured relative to the reference electrode. I used a computer controlled, pulse deposition to create the bilayers of copper and cobalt inside the membrane pores. The electrolyte contained both Cu and Co ions with boric acid to buffer the solution to the correct pH. Co deposits at a lower potential than Cu and as a consequence, Cu is codepositing. This difficulty is overcome by making the concentration of Co 80 times higher than that of the Cu in order to minimize Cu impurities. The total amount of charge is counted by integrating the current. The effective deposition area and bulk densities of the materials are known so a thickness can be correlated to an amount of charge. In this way an effective method of creating tailored nanowire geometries is obtained. Depending on pore diameter, the wires are between 6 and 10 microns in length. The top of the membrane is then capped with Cu inside the sputtering chamber. The sample is then ready for magnetometry measurements but magnetoresistance measurements require more processing. In order to gain an appreciable resistance value a small number of wires needed to be isolated. The pore density of the membranes is $3 - 6 \times 10^8 wires/cm^2$ or $3 - 6 wires/\mu m^2$ so to isolate a small number of wires is not a trivial task. As shown in FIG. 3 a small piece of the sample is masked with a thin strip on top and another thin strip, perpendicular to the top strip, on the bottom. The unmasked Cu is etched away in a chemical etchant and where the remaining strips cross there is a small area of connected wires. I then attached voltage and current leads to the top and bottom of the sample to measure resistance. I attached these samples to small chips connected to either a lock-in amplifier or a digital voltmeter/constant current source. This chip was suspended between an electromagnet to make GMR measurements.
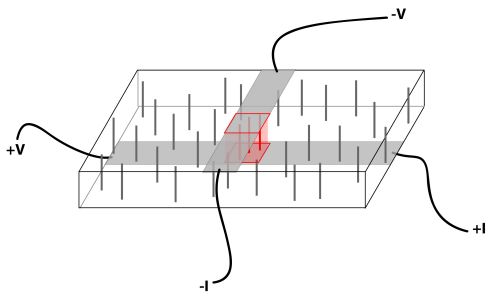

FIG. 3: Four Point Connection

IV. RESULTS

I fabricated 50nm diameter wires with Co thicknesses of 1nm to 5nm and Cu thicknesses from 1nm to 21nm. The value of GMR is measured relative to the saturation resistance

$$MR = \frac{R_{Max} - R_{Sat}}{R_{Sat}} \times 100\%$$

. The maximum MR value obtained was for Co 5nm thick spaced by 8nm layers of Cu with a value of 8 At
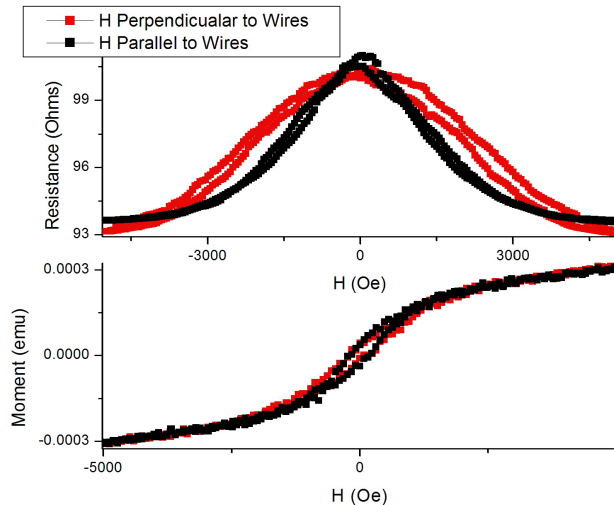

FIG. 4: Single Domain GMR and Moment Data for $[Co5nm/Cu8nm]_{400bilayers}^{d=50nm}$

these domain sizes an isolated disk undergoes single domain reversal and the GMR signature is fairly well understood. I then fabricated samples with cobalt thicknesses of 40nm to 60nm and copper thicknesses of 10nm in 200nm membranes. According to earlier studies undertaken in the Liu Lab, isolated disks at this size undergo vortex state reversal[8]. However, multilayer stacks of interacting disks have not been studied comprehensively. A study of how vortex state disks interact magnetostatically in a plane is conducted in [9] and [10]. Magnetostatic interactions tend to lower the absolute value of the nucleation and annihilation fields of the vortex state disks. In [11] trilayer systems with vortex states separated vertically by 20nm of copper are studied. These systems have the interesting property that one layer nucleates first and strongly effects the entire vortex evolution of the other disk including the position of vortex nucleation and the path traveled by the vortex core. These effects hint at magnetic properties of the layered nanowires I created.

As shown in [12] interlayer coupling and dipolar interactions can completely dominate magnetic anisotropy effects, masking the magnetic signatures of the individual disks. Using a vibrating sample magnetometer (VSM) [8] Wong has found that vortex state transitions happen in *isolated* disks fabricated in the same method and sizes as my nanowires. However, when VSM techniques are used to explore my interacting disks of the same dimensions as [8], the FORC signatures show no correlation.

This is attributed to the interlayer coupling and dipolar interactions within the wires. The stacked geometry of the multilayered wires with buried interfaces makes alternate magnetic measurement techniques, such as optical or neutron techniques, inadequate for exploring this magnetic configuration. Therefore I modified the VSM operating system to control a digital current source, voltmeter, and lock-in amplifier so measurements of both AC and DC GMR are possible. Using this new capability I analyzed a sample, $[Co50nm/Cu10nm]_{150bilayers}^{d=200nm}$ presumed to contain vortex state disks. This sample has interesting GMR results shown in FIG. 5 . This signal
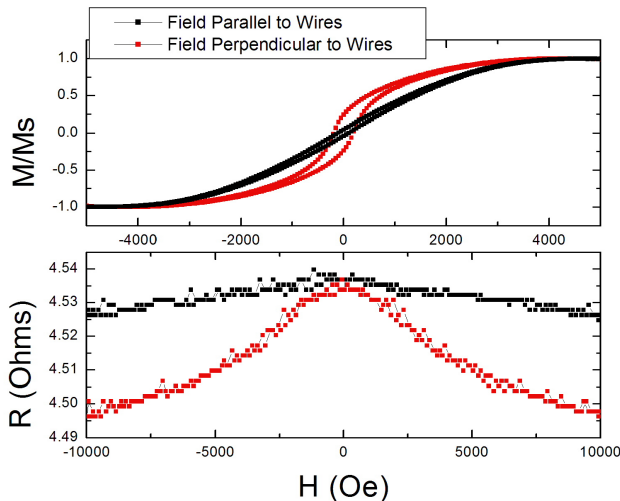

FIG. 5: Possible Vortex Sate GMR Signal $[Co50nm/Cu10nm]_{150bilayers}^{d=200nm}$

shows a standard MR signal with the field in the plane of the disks but shows an anomalous signal for the out of plane direction. Additionally there is a noticeable drop in resistance for very small field values that may be an anisotropic magnetoresistance signal originating form the vortex cores of the disks. This result indicates that magnetoresistance measurements probe the magnetic configurations of samples. I also studied a current-in-plane giant magnetoresistance sample (CIP-GMR) fabricated by Randy Dumas. This sample was more stable and thus I could preform GMR FORCs on it shown in FIG. 6. One can see from the data that higher resistance states are accessed from inside the major hysteresis loops hinting that a higher spin disorder state is being probed. This merits further study.

V.   CONCLUSION

In conclusion, I learned a new programing language and automated an instrument to add new measurement capabilities to the lab. I fabricated many nanowire sam-
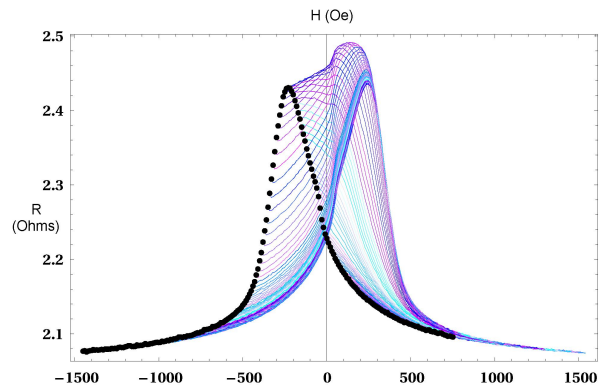

FIG. 6: Resistance FORC on CIP-GMR Sample

ples and analyzed their magnetic and magnetoresistance properties. I also attempted to correlate GMR signals with magnetic configuration with varying degrees of success.

VI.   ACKNOWLEDGEMENTS

* Electronic address: Peter.K.Greene@gmail.com
† Department of Physics REU Program Summer 2007, University of California, Davis, California, 95616

[1] C. Kittel, Rev. Mod. Phys. **21**, 541 (1959).
[2] S. Blundell, *Magnetism in Condensed Matter* (Oxford University Press, NewYork, 2001).
[3] M. N. Baibich, J. M. Broto, A. Fert, F. N. V. Dau, F. Petroff, P. Eitenne, G. Creuzet, A. Friederich, and J. Chazelas, Phys. Rev. Lett. **61**, 2472 (1988).
[4] G. Binasch, P. Grunberg, F. Saurenbach, and W. Zinn, Phys. Rev. B **39**, 4828 (1989).
[5] S. S. P. Parkin, R. Bhadra, and K. P. Roche, Phys. Rev. Lett. **66**, 2152 (1991).
[6] T. Valet and A. Fert, Phys. Rev. B **48**, 7099 (1993).
[7] K. Liu, *Doctoral Dissertation: Magnetism and Magneto-Transport in Systems with Different Dimensions* (Johns Hopkins University, 1998).
[8] J. Wong, *Senior thesis*, unpublished (2006).
[9] V. Novosad, K. Y. Guslienko, Y. Otani, H. Shima, and K. Fukamichi, J. Magn. Magn. Mater. **236**, 234 (2002).
[10] H. Shima, K. Y. Guslienko, V. Novosad, Y. Otani, K. Fukamachi, N. Kikuchi, O. Kitakami, and Y. Shimada, J. Appl. Phys. **91**, 6952 (2002).
[11] K. S. Buchanan, K. Y. Guslienko, A. Doran, A. Scholl, S. D. Bader, and V. Novosad, Phys. Rev. B **72**, 134415 (2005).

[12] L. Carignan, C. Lacroix, A. Ouimet, M. Ciureanu, A. Yelon, and D. Menard, J. Appl. Phys. **102**, 023905 (2007).